Syntheses and photophysical properties of type-II CdSe/ZnTe/ZnS (core/shell/shell) quantum dots†

Chiu-Ting Cheng,[a] Chun-Yen Chen,[a] Chih-Wei Lai,[a] Wei-Hsin Liu,[a] Shih-Chieh Pu,[a] Pi-Tai Chou,*[a] Yi-Hsuan Chou[b] and Hsin-Tien Chiu*[b]

Received 11th March 2005, Accepted 29th June 2005
First published as an Advance Article on the web 15th July 2005
DOI: 10.1039/b503681j

Syntheses of CdSe/ZnTe/ZnS (core/shell/shell) type-II quantum dots (QDs) are reported. Structural characterization was made *via* TEM, EDX, XPS and XRD. Photophysical properties were investigated *via* the interband emission (CdSe → ZnTe) and its associated quantum efficiency as well as relaxation dynamics. In comparison to the weak emission ($\Phi_f \sim 4 \times 10^{-3}$ in toluene) of CdSe/ZnTe (3.9/0.5 nm), capping ZnS (0.4 nm in thickness) enhances the CdSe → ZnTe interband emission by ~30 fold ($\Phi_f \sim 0.12$), whereas the peak wavelength shifts only slightly to the red. By encapsulating dihydrolipoic acid (DHLA), water-soluble CdSe/ZnTe/ZnS QDs were also prepared, and they exhibited an interband emission at ~930 nm with an emission yield of ~0.1. Femtosecond pulse excitation ($\lambda_{ex} \sim 1200$ nm) measurement estimated a two-photon absorption cross section, σ, of $\sim 70 \times 10^{-50}$ cm^4 s photon^{-1} for DHLA-capped CdSe/ZnTe/ZnS in water, supporting its suitability for the use as near-infrared (NIR) dyes in biomedical imaging.

Introduction

Type-II quantum dots (QDs) have both valence and conduction bands in the core lower (or higher) than those in the shell materials. After electronic excitation, one carrier is predominantly confined to the core, while the other is located at the shell. This spatial separation of charge carriers leads to several characteristic differences from the type-I QDs. Particularly, the interband emission is allowable with an energy gap that would be otherwise inaccessible with type-I structures, extending the color-tuning capability even to the near-IR. However, despite well-documented studies of type-I core/shell QDs,[1–7] studies of type-II QDs are relatively rare. Recently, based on a colloidal template, a seminal work on the chemical syntheses of type-II CdTe/CdSe (core/shell) and CdSe/ZnTe (core/shell) QDs using $Cd(CH_3)_2$ as a Cd precursor has been reported.[8] This colloidal template approach is crucial in that it provides both feasibility and versatility toward further chemical modification. Subsequently, we have reported the synthesis of CdSe/ZnTe (core/shell) type-II QDs *via* a safer precursor, CdO, and studied their corresponding excited-state relaxation dynamics.[9] In another approach, CdTe/CdSe type-II QDs have been exploited as near-infrared (NIR) dyes for biomedical imaging in living tissue by taking advantage of their great photostability and deeper light penetration.[10] In view of applications, one disadvantage to using type-II QDs, however, lies in their much weaker quantum efficiency in general relative to type-I QDs. Since the interband emission originates from the spatially separated CdSe → ZnTe transition, its associated radiative lifetime is expected to be long. Thus, any radiationless process, such as the floating of hole-carriers to the surface in the case of CdSe/ZnTe QDs, will drastically quench the emission intensity. As an approach to enhancing the quantum efficiency toward NIR applications, we report herein the encapsulation of a third layer with ZnS to achieve a CdSe/ZnTe/ZnS (core/shell/shell) structure. As shown in Scheme 1, in this case, the conduction band in ZnTe

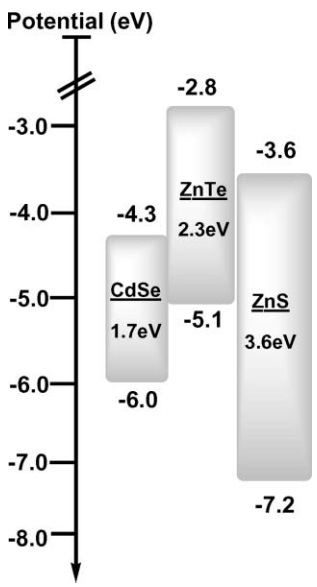

Scheme 1 Plot illustrating the CdSe, ZnTe and ZnS band offsets alignment in energy (data are taken from ref. 11). Note that the changes of band gap and hence the relative energies in the interfacial regions are neglected in this diagram.

[a]*Department of Chemistry, National Taiwan University, Taipei 106, Taiwan. E-mail: chop@ntu.edu.tw; Fax: 886-2-23695208; Tel: 886-2-23630231 ext.3988*
[b]*Department of Applied Chemistry, National Chiao Tung University, Hsinchu 300, Taiwan*

† Electronic supplementary information (ESI) available: Fig. S1: XPS spectra of CdSe/ZnTe and CdSe/ZnTe/ZnS QDs. See http://dx.doi.org/10.1039/b503681j

is well above that in CdSe, while the valence band of ZnS is below that of ZnTe. Upon excitation, electrons and holes are strictly confined in CdSe and ZnTe, respectively, encapsulated by ZnS. Thus, floating of hole-carriers to the surface (ZnS) can be significantly reduced, resulting in the enhancement of CdSe → ZnTe interband emission intensity.

Structural characterization of the synthesized CdSe/ZnTe/ZnS QDs has been made *via* TEM, EDX, XPS and XRD. Photophysical properties were investigated *via* the absorption, interband emission (CdSe → ZnTe) and its associated quantum efficiency, as well as relaxation dynamics. In view of applications in biomedical imaging, dihydrolipoic acid (DHLA) encapsulated water-soluble CdSe/ZnTe/ZnS QDs were also prepared and the corresponding two-photon cross section was measured. Details of results and discussion are elaborated as follows.

Experimental

Chemicals

Tri-*n*-octylphosphine oxide (TOPO, 99%, Aldrich), tri-*n*-butylphosphine (TBP, technical grade 98%, SHOWA), di-*n*-octylamine (DOA, 98%, ACROS), hexadecylamine (HDA, 90%, TCI), CdO (99.99%, Strem), selenium (Se) powder 200 mesh (99.5%, Aldrich), sulfur (S) powder (99.5%, Aldrich), tellurium (Te) powder (99.8%, 200 mesh, Aldrich) and zinc stearate (Riedel-deHaën) were used immediately after receipt.

Preparation procedures

The CdSe/ZnTe core/shell nanoparticles were prepared according to our previous report.[9] To obtain the CdSe/ZnTe/ZnS core/shell/shell nanoparticles, the precipitated CdSe/ZnTe QDs (0.020 g) were dispersed in TOPO (2.20 g) and HDA (1.26 g) before being heated to 190 °C. In addition, Zn stearate (0.316 g) was dissolved in 2.5 mL of TBP upon gentle heating (*ca*. 80 °C). After being cooled to room temperature, the resulting 0.2 M solution was mixed with 2.5 mL of a 0.2 M solution of S in TBP. With a syringe pump, this mixture was injected within 1 h into the reaction flask containing the core/shell nanocrystals at 190–200 °C. After the addition was complete, the crystals were annealed at 190 °C for an additional 1–1.5 h. CdSe/ZnTe/ZnS QDs of various ZnS thicknesses could be obtained by adjusting the concentrations of Zn stearate and S in TBP as well as the corresponding injection times. The resulting CdSe/ZnTe/ZnS QDs were further purified by centrifugation and re-precipitating twice from methanol.

The water-soluble CdSe/ZnTe/ZnS nanoparticles were prepared using a stepwise procedure reported by Mattoussi *et al.*[12] with a slight modification. Briefly, TBP/TOPO-capped CdSe/ZnTe/ZnS core/shell/shell particles were subsequently exchanged with 20 mg DHLA (freshly prepared from distilled thioctic acid by sodium borohydride reduction)[13] placed in a reaction vessel. 15 mL of methanol was added, and the pH was adjusted to >10 with tetramethylammonium hydroxide pentahydrate. Under dark conditions, 10 mg of CdSe/ZnTe/ZnS nanocrystals were dissolved in the mixture, and the vessel was placed under a regular airflow. The mixture was heated under reflux at 65 °C overnight, and then the reaction was terminated and the mixture allowed to cool to room temperature. The DHLA-capped nanocrystals were then precipitated with diethyl ether. For further purification, methanol was added to dissolve the precipitate, followed by the addition of diethyl ether to reprecipitate the nanocrystals.

Measurements

The sizes of the QDs were determined with a Hitachi H-7100 transmission electron microscope (TEM). Further characterization of QDs was made by powder X-ray diffraction (XRD, model PANalytical X′ Pert PRO) and X-ray photoelectron spectroscopy (XPS, model VG Scientific ESCALAB 250). UV-Vis steady-state absorption and emission spectra were recorded with a Hitachi (U-3310) spectrophotometer and an Edinburgh (FS920) fluorimeter, respectively. The NIR emission spectra were obtained by exciting the sample solution under a front-face excitation configuration using an Ar ion laser (488 or 514 nm, Coherent Innova 90). The emission was then sent through an NIR-configured Fourier-transform interferometer (Bruker Equinox 55) and detected with an NIR sensitive photomultiplier (Hamamatsu model R5509-72) operated at −80 °C. Details of nanosecond lifetime measurements have been described previously.[9] IR125 (Exciton) was used as a standard for the quantum yield (Φ_f) measurement. Φ_f for IR125 was reported to be 0.11 in dimethyl sulfoxide (emission peak wavelength ~910 nm).[14]

For the measurement of the two-photon absorption cross section, a mode-locked femtosecond Ti:Sapphire laser (Spectra-physics, 100 fs, 80 MHz) pumped Opal (Spectra-physics, 130 fs, 80 MHz) was used as the excitation source. The NIR fluorescence was collected at a direction perpendicular to the pump beam. To minimize the re-absorption effect, the excitation beam was focused as closely as possible to the front wall of the quartz cell. The near-infrared (NIR) emission was measured by a photomultiplier tube (Hamamatzu R5509-72) coupled with a Lock-in Amplifier (Stanford Research System SR830) and a monochromator (Acton, SpectraPro-275) in that the grating was blazed at 1200 nm. The dye 5,10,15,20-tetraphenylporphine (H_2TPP, Aldrich) was used as a standard, for which the two-photon absorption cross section (σ) was reported to be 3.5 GM (1 GM = 10^{-50} cm^4 s photon^{-1}) upon 1200-nm excitation in toluene.[15]

Results and discussion

Fig. 1 depicts TEM images and size histograms of CdSe/ZnTe (core/shell) and CdSe/ZnTe/ZnS (core/shell/shell) in which the core/shell (CdSe/ZnTe) QDs are from the same batch. The size histograms of CdSe/ZnTe and CdSe/ZnTe/ZnS QDs were established *via* counting each individual size for 500 particles. Since the CdSe/ZnTe/ZnS QDs were prepared from the same batch of CdSe/ZnTe, it is reasonable to assume the same core/shell size. As an indirect approach, the thickness of ZnS can be estimated by the subtraction of CdSe/ZnTe size from that of the CdSe/ZnTe/ZnS prepared. For the QDs shown in Fig. 1, the diameters of CdSe/ZnTe and CdSe/ZnTe/ZnS were measured to be in an average of 5.0 and 5.8 nm, respectively. Accordingly, the thickness of ZnS was estimated to be 0.4 nm.

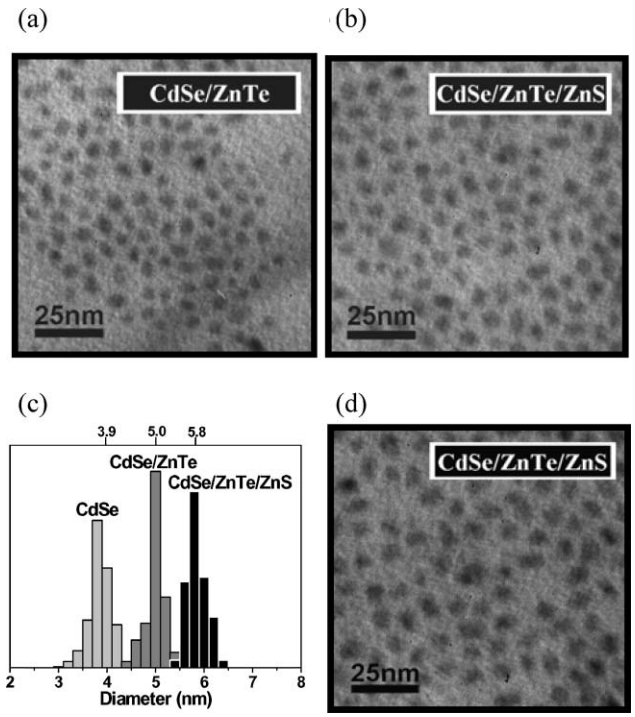

Fig. 1 TEM images of the samples with average diameter of 5.0 nm for CdSe/ZnTe QDs (a) and 5.8 nm for CdSe/ZnTe/ZnS QDs (b). (c) Size histograms for the samples in which the histograms were constructed by counting 500 particles in each sample. (d) CdSe/ZnTe/ZnS QDs of 6.6 nm (0.8 nm thickness in ZnS).

Considering that TEM generally provides insufficient contrast at the edges of nanoparticles, the calculated ZnS thickness could be subject to ~10–15% uncertainty.

The corresponding composition of CdSe/ZnTe/ZnS QDs was characterized by energy dispersive spectroscopy (EDX). As shown in Fig. 2(a), the appearance of the S peak at 2.33 keV, in combination with the increase of the ratio for Zn *vs.* Te from CdSe/ZnTe to CdSe/ZnTe/ZnS, may indirectly support the formation of the ZnS shell, although the possibility of alloy formation can not be ruled out. Furthermore, as shown in Fig. 2(b), comparing the XRD pattern of the CdSe/ZnTe core/shell, two sets of peaks at faces (100), (002), (101) and (110), (103), (112) in CdSe/ZnTe/ZnS QDs revealed the same spectral features, with a slight shift to lower scattering angle for the (110), (103), (112) peaks. Owing to a similar XRD pattern for these two sets of peaks, the formation of an alloy upon encapsulating ZnS is not likely. Nevertheless, similar to the results of EDX, the X-ray data could not definitely conclude a core/shell/shell structure.

In an attempt to extract more composition information we have further made efforts to perform XPS analyses. However, as depicted in the ESI,† our results revealed negligibly small differences in XPS peaks between CdSe/ZnTe and CdSe/ZnTe/ZnS systems for Cd, Zn, Se and Te elements. Such results may not be surprising; for the case of Cd $3d_{5/2}$ in CdSe and CdTe, photoelectron peaks are expected to be located at 404.8 eV[16] (or 405.0 eV[17]) and 405.0 eV[16] (or 404.8 eV[17]), respectively. Our results of ~405.4 eV, within experimental uncertainty, can not be definitely distinguished. Alternatively,

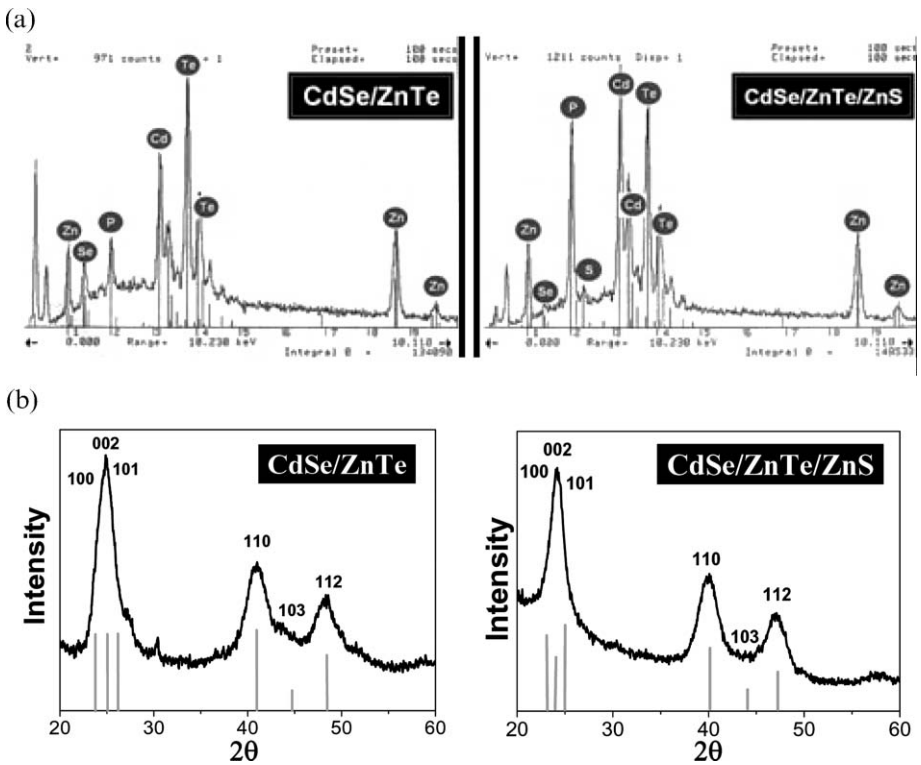

Fig. 2 (a) Energy dispersive spectroscopy (EDX) characterization of CdSe/ZnTe core/shell QDs (left) and CdSe/ZnTe/ZnS core/shell/shell QDs. (b) X-Ray diffraction (XRD) data of CdSe/ZnTe core/shell QDs (left) and CdSe/ZnTe/ZnS core/shell/shell QDs (right).

if one focuses on the Te $3d_{5/2}$ state, the resulting Te peak was located at 572.8 eV for both CdSe/ZnTe and CdSe/ZnTe/ZnS systems (see ESI†). In comparison, the corresponding peak for ZnTe is expected to be at 572.9 eV,[18] which is similar to that of CdTe of 572.7 eV.[18] Thus, the resolution of our current system is not sufficiently high enough to resolve the origin of the 572.8 eV peak. Similarly, the Zn $2p_{3/2}$ signal in ZnTe, predicted to be at 1021.4 eV,[16] is also indistinguishable from that of ZnS (1021.4 eV[16]), so that our result of ~1021.4 eV can not be unambiguously assigned to either. Nevertheless there is no signal at 1022.0 eV[17] for ZnSe, the results of which, in part, support the lack of alloy formation between CdSe and ZnTe layers in the CdSe/ZnTe/ZnS system.

In the angle-resolved XPS approach, the peak intensity ratio for elements of the core and the shell as a function of the electron takeoff angle may serve as a tool for extracting geometrical information about the nanoparticles.[19] For example, Piyakis *et al.*[20] have reported the XPS analysis of spherical Cu nanoclusters by using angle-resolved XPS in combination with Monte Carlo simulation.[20] We have thus made extensive efforts in the angle-tuning studies. Unfortunately, negligible electron-takeoff-angle dependence was observed for the ratio of peak intensities. This result can be tentatively rationalized by the rather thin layer for both the ZnTe (0.5 nm) and ZnS (0.4 nm) shell in comparison to the CdSe core (3.9 nm in diameter), so that the peak intensities for Zn and Te (or S) in the two shell layers are not sensitive enough to the angle tuning. Consequently, in the following section. we will focus on absorption and luminescence spectroscopy to substantially support our viewpoint of CdSe/ZnTe/ZnS formation.

The absorption and emission spectra of the three types of QDs are shown in Fig. 3. Apparently, despite the significant differences in absorption and emission spectra from CdSe (λ_{em} ~ 570 nm) to CdSe/ZnTe (λ_{em} ~865 nm), only slight red shifting in both absorption and emission spectral features was observed from CdSe/ZnTe to CdSe/ZnTe/ZnS (λ_{em} ~915 nm). Note that in general an alloy composite would give a blue shift in both emission and absorption edge.[21] Thus, the red shift in both absorption and emission spectra indirectly proves the CdSe/ZnTe/ZnS (core/shell/shell) structure rather than alloy formation. Furthermore, it seems unlikely that ZnTe and ZnS would form an alloy because of their lattice mismatch (the CdSe lattice (6.05 Å) is about 12% larger than that of ZnS (5.41 Å).[21] The resulting emission energy gap may be rationalized by the energy diagram depicted in Scheme 1, although the corresponding energetics refer to the bulk materials. As depicted in Scheme 1, the lowest energy gap should be ascribed to the ZnTe → CdSe interband transition (~0.8 eV), while the interband transition between ZnTe and ZnS is much higher in energy (~1.5 eV) and may have negligible influence on the lower lying transitions.

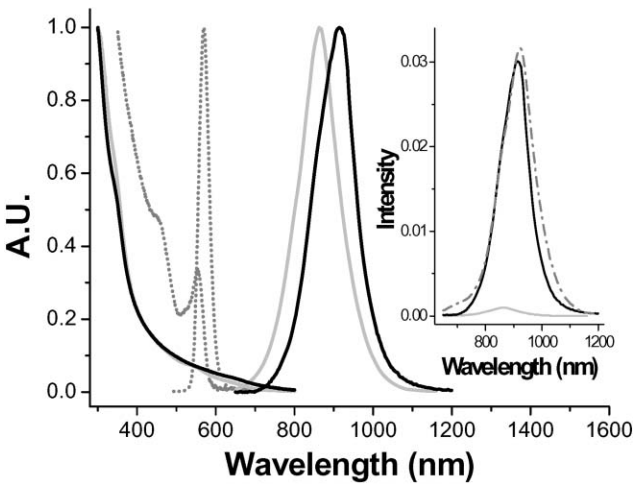

Fig. 3 The normalized absorption and emission spectra of the CdSe core QDs (3.9 nm, dotted line), CdSe/ZnTe core/shell QDs (5.0 nm, light grey) and CdSe/ZnTe/ZnS core/shell/shell QDs (5.8 nm, black) QDs in toluene; see Table 1 for the corresponding diameters. Inset: The emission intensity of CdSe/ZnTe/ZnS QDs (black: 5.8 nm, dashed line: 6.6 nm) *vs*, that of CdSe/ZnTe QDs (5.0 nm, light grey) under identical experimental conditions.

Table 1 lists the room-temperature emission properties for all three types of QDs with the same core size (and same thickness for ZnTe). While CdSe gave rise to a ligand (TOPO) confined 570-nm emission with quantum efficiency as high as 0.52, the CdSe/ZnTe 865-nm emission is relatively much weaker, with a quantum yield (Φ_f) estimated to be 4.0×10^{-3}. Lifetimes (τ_f) for CdSe and CdSe/ZnTe were further measured to be 35 and 55 ns, respectively. The radiative decay rates, k_r, calculated according to $k_r = \Phi_f/\tau_f$, were then deduced to be 1.5×10^7 s^{-1} (CdSe) and 7.3×10^4 s^{-1} (CdSe/ZnTe). Accordingly, the nonradiative decay rates were deduced to be 1.4×10^7 s^{-1} and 1.8×10^7 s^{-1} for CdSe and CdSe/ZnTe, respectively. The ~200-fold smaller radiative lifetime for the CdSe → ZnTe emission is attributed to the spatially separated electron–hole recombination. As a result, despite the same magnitude of radiationless decay rates in CdSe/ZnTe QDs, its quantum efficiency is much lower than that of CdSe.

A drastic increase of the CdSe → ZnTe interband emission intensity was observed after encapsulating ZnS. The quantum efficiency was increased to 0.12, which is ~30 times as large as that of the CdSe/ZnTe QDs. More importantly, the peak wavelength, *i.e.* the associated CdSe → ZnTe energy gap, changed only slightly, with a slight bathochromic shift from 865 to 915 nm, and hence an energy shift of ~1.8 kcal mol^{-1}. The small variation of the peak wavelength also supports the aforementioned viewpoint that coating ZnS only affected slightly the CdSe → ZnTe transition due to the well separated upper and lower energy levels in the conduction and valence bands, respectively, for ZnS. The increase of quantum efficiency also correlates well with the increase of the observed lifetime to as large as ~1.2 μs. Accordingly, the radiative

Table 1 Room-temperature photophysical properties for CdSe, CdSe/ZnTe and CdSe/ZnTe/ZnS QDs

	Size/nm	PL (λ_{max})/nm	τ_f/ns	Φ_f
CdSe[a]	3.9	570	35	0.52
CdSe/ZnTe[a]	5.0	865	55	0.004
CdSe/ZnTe/ZnS[a]	5.8	915	1200	0.12
CdSe/ZnTe/ZnS[a]	6.6	920	1210	0.12
CdSe/ZnTe/ZnS[b]	—[c]	930	950	0.10

[a] TOPO-capped QDs in toluene. [b] DHLA-capped QDs in water (pH ~ 7.0), [c] Not available due to the aggregation, see text.

decay rate was calculated to be 1.0×10^5 s^{-1}, which, within experimental error, is similar to that of CdSe/ZnTe, indicating negligible interference from ZnS; rather, ZnS plays a key role in introducing a barrier to confine holes in ZnTe (see Scheme 1). This viewpoint can be further supported by the deduced radiationless decay rate of 7.3×10^5 s^{-1}. The rather small radiationless decay rate constant in CdSe/ZnTe/ZnS QDs is plausibly due to the hole trapping in ZnTe so that fewer holes are present on the outer surface. We further made a synthetic attempt to increase the thickness of ZnS from ~0.4 to ~0.8 nm. The increase of average size from ~5.8 to 6.6 nm can be seen from Fig. 1(d). As depicted in the inset of Fig. 3, the emission peak wavelength only slightly shifted from 915 nm (0.4 nm ZnS) to 920 nm (0.8 nm ZnS), with <3% increase of quantum efficiency (see Table 1). Further increase of ZnS thickness to ~1.1 nm resulted in negligible changes for both peak wavelength and emission intensity (not shown here), indicating that ZnS with a thickness of ⩾0.4 nm should have a good passivation on ZnTe.

Fig. 4 shows the 930-nm emission (Φ_f ~0.10) of water-soluble, *i.e.* DHLA-capped, CdSe/ZnTe/ZnS QDs. In comparison to its precursor, *i.e.* TOPO-capped CdSe/ZnTe/ZnS QDs (λ_{max} ~915 nm in toluene), the ~15 nm bathochromic shift of the emission peak is possibly due to the perturbation of different solvent polarities. Nevertheless, one can not eliminate subtle changes of size distributions during chemical modification. Unfortunately, TEM revealed aggregation of DHLA-capped CdSe/ZnTe/ZnS QDs, which prevented further differentiation between the TOPO- and DHLA-capped QDs in size distribution. Measurements of the two-photon absorption cross section were carried out by femtosecond pulse excitation (λ_{ex} ~1200 nm, 130 fs). The spectral feature of the emission upon 1200-nm excitation was qualitatively the same as that of one-photon excitation (see Fig. 5). As shown in Fig. 5, the plot of 930-nm peak intensity *vs.* the square of excitation power

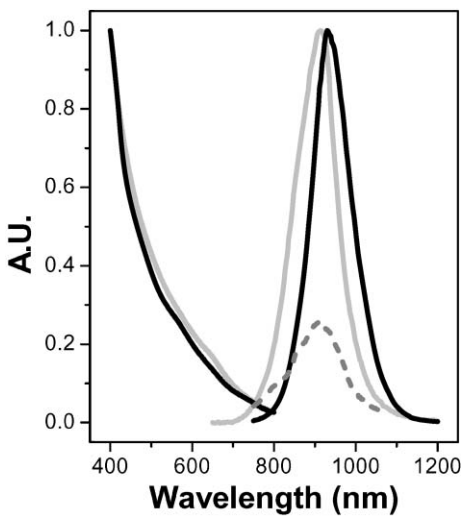

Fig. 4 The absorption and emission spectra (light grey) of TOPO-capped CdSe/ZnTe/ZnS QDs **a** in toluene and of DHLA-capped CdSe/ZnTe/ZnS QDs in water (pH ~7) (black) synthesized from batch **a**. The dashed curve shows the emission of DHLA-capped CdSe/ZnTe/ZnS QDs in water excited by 1200-nm laser pulses.

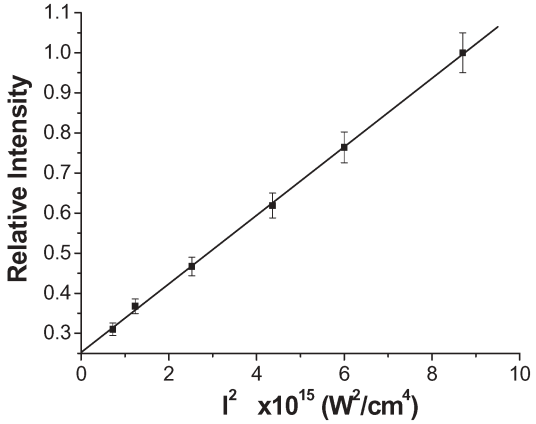

Fig. 5 Plot of 930-nm peak intensity (I) for DHLA-capped CdSe/ZnTe/ZnS as a function of the square of excitation power (λ_{ex} ~ 1200 nm).

showed sufficiently linear behavior, supporting the origin of emission from a two-photon absorption process.

Taking the absorption extinction coefficient for CdSe (3.9 nm) to be 2.2×10^5 $M^{-1}cm^{-1}$,[22] the DHLA-capped CdSe/ZnTe/ZnS concentration was calculated as 5.8×10^{-7} M in this study. Upon preparing the same concentration for both DHLA-capped CdSe/ZnTe/ZnS QDs and H_2TPP, the two-photon excited emission intensity for DHLA-capped CdSe/ZnTe/ZnS QDs was calculated to be ~20-fold higher than that of H_2TPP. Knowing σ to be 3.5 GM for H_2TPP,[15] σ for CdSe/ZnTe/ZnS QDs was estimated to be ~70 GM.

Conclusion

In conclusion, synthesis of CdSe/ZnTe/ZnS (core/shell/shell) type-II QDs from CdSe/ZnTe has been achieved. In comparison to that of type-II CdSe/ZnTe, although the addition of ZnS only changed the interband emission peak wavelength slightly, due to the quantum confinement for the CdSe → ZnTe interband emission, type-II CdSe/ZnTe/ZnS gives rise to ~30-fold enhancement of the quantum efficiency (Φ_f ~0.12). By encapsulating DHLA, water-soluble CdSe/ZnTe/ZnS (3.9/0.5/0.4 nm) was prepared, and such QDs exhibited an interband emission at ~930 nm with a fluorescence yield of ~0.1. Femtosecond pulse (λ_{ex} ~1200 nm) excitation measurement derives a two-photon absorption cross section, σ, of ~70 GM for the latter QDs, supporting their suitability for use as near-IR dyes for biomedical imaging by taking advantage of their great photostability and deep light penetration.

References

1 A. P. Alivisatos, *Science*, 1996, **271**, 933.
2 M. Danek, K. F. Jensen, C. B. Murray and M. G. Bawendi, *Chem. Mater.*, 1996, **8**, 173.
3 B. O. Dabbousi, J. Rodriguez-Viejo, F. V. Mikulec, J. R. Heine, H. Mattoussi, R. Ober, K. F. Jensen and M. G. Bawendi, *J. Phys. Chem. B*, 1997, **101**, 9463.
4 M. Nirmal and L. Brus, *Acc. Chem. Res.*, 1999, **32**, 407.
5 H. Mattoussi, J. M. Mauro, E. R. Goodman, G. P. Anderson, V. C. Sundar, F. V. Mikulec and M. G. Bawendi, *J. Am. Chem. Soc.*, 2000, **122**, 12142.

6 D. V. Talapin, A. L. Rogach, A. Kornowski, M. Haase and H. Weller, *Nano Lett.*, 2001, **1**, 207.
7 P. Reiss, J. Bleuse and A. Pron, *Nano Lett.*, 2002, **2**, 781.
8 S. Kim, B. Fisher, H. J. Eisler and M. G. Bawendi, *J. Am. Chem. Soc.*, 2003, **125**, 11466.
9 C. Y. Chen, C. T. Cheng, J. K. Yu, S. C. Pu, Y. M. Cheng, P. T. Chou, Y. H. Chou and H. T. Chiu, *J. Phys. Chem. B*, 2004, **108**, 10687.
10 S. Kim, Y. T. Lim, E. G. Soltesz, A. M. De Grand, J. Lee, A. Nakayama, J. A. Parker, T. Mihaljevic, R. G. Laurence, D. M. Dor, L. H. Cohn, M. G. Bawendi and J. V. Frangioni, *Nat. Biotechnol.*, 2004, **22**, 93.
11 S. J. Pearton, *Wide Bandgap Semiconductors*, William Andrew Publishing, New York, 2000, p. 9.
12 H. Mattoussi, J. M. Mauro, E. R. Goldman, G. P. Anderson, V. C. Sundar, F. V. Milkulec and M. G. Bawendi, *J. Am. Chem. Soc.*, 2000, **122**, 12142.
13 I. C. Gunsalus, L. S. Barton and W. Gruber, *J. Am. Chem. Soc.*, 1956, **78**, 1763.
14 R. C. Benson and H. A. Jues, *J. Chem. Eng. Data.*, 1977, **22**, 379.
15 A. Karotki, M. Drobizhev, M. Kruk, C. Spangler, E. Nickel and N. Mamardashvili, *J. Opt. Soc. Am. B*, 2003, **20**, 321.
16 D. Briggs and M. P. Seah, *Practical surface analysis by Auger and X-ray photoelectron spectroscopy*, John Wiley & Sons, New York, 2nd edn., 1993, vol. 1.
17 C. D. Wagner, W. M. Riggs, L. E. Davis, J. F. Moulder and G. E. Muilenberg, *Handbook of X-Ray Photoelectron Spectroscopy*, Physical Electronics Division, Perkin-Elmer Corporation, Minnesota, 1979.
18 H. Ebert, M. Knecht, M. Muhler, O. Helmer and W. Bensch, *J. Phys. Chem.*, 1995, **99**, 3326.
19 I. Tunc, S. Suzer, M. A. Correa-Duarte and L. M. Liz-Marzan, *J. Phys. Chem. B*, 2005, **109**, 7597.
20 K. N. Piyakis, D.-Q. Yang and E. Sacher, *Surf. Sci.*, 2003, **536**, 139.
21 M. A. Malik, P. O'Brien and N. Revaprasadu, *Chem. Mater.*, 2002, **14**, 2004.
22 W. W. Yu, L. Qu, W. Guo and X. Peng, *Chem. Mater.*, 2003, **15**, 2854.